

Theoretical analyses for a 2-2 cement-based piezoelectric curved composite with electrode layers

Taotao Zhang*

School of Transportation Science and Engineering, Beihang University, Beijing, 100191, P. R. China

(Received February 28, 2014, Revised September 22, 2014, Accepted September 23, 2014)

Abstract. Based on the general theory of elasticity, the static behavior of 2-2 cement-based piezoelectric curved composites is investigated. The actuator consists of 2 cement layers and 1 piezoelectric layer. Considering the electrode layer between the cement layer and the piezoelectric layer as the elastic layer, the exact solutions of the mechanical and electrical fields of the curved composites are obtained by utilizing the Airy stress function method. Furthermore, the theoretical results are compared with the FEM results and good agreements (with almost no error) are obtained, thus proving the validity of this study. Furthermore, the influence of certain parameters is discussed, which can help to get the desired displacements and stresses. Finally, it is seen that the analytical model established in this paper works well, which could benefit the design of this kind of cement-based smart devices.

Keywords: 2-2 cement based; piezoelectricity; curved composite; theoretical solutions; actuator; electrode layers

1. Introduction

A cement-based piezoelectric composite has excellent piezoelectric properties and good compatibility with concrete in civil engineering structures; moreover, it shows more benefit for measuring the properties of the civil engineering structures than other smart materials. Therefore, more and more efforts are being devoted in the preparation of cement-based piezoelectric composites and their applications in Civil Engineering. To meet the requirement of concrete civil engineering structures, Li *et al.* (2002) have fabricated the 0-3 cement-based piezoelectric composite by the normal mixing and spreading method for the first time in the field of piezoelectric materials. Preliminary results showed that the composite is effective and applicable in both piezoelectric properties and compatibility, and can be utilized to fabricate cement-based sensors for applications in concrete structures. Zhang *et al.* (2002a) have discussed the feasibility of the fabrication, polarization and adjustability of the acoustic impedance of the cement-based piezoelectric smart composites. They have showed that by using the cement-based materials as the matrix of the piezoelectric smart composites, the problems of the mismatch and fabrication as well as reducing the polarization voltage could be solved. With the dice-and-fill technique, Xu *et al.* (2009) have fabricated the 2-2 type cement based piezoelectric composites, which has wider

*Corresponding author, Dr., E-mail: zhangtt@buaa.edu.cn

frequency band and higher sensitivity to be used as transducers. They have also analyzed the effects of the cement matrix and composite thickness on the electrical and acoustic properties of the 2-2 type cement-based piezoelectric composites (Xu *et al.* 2011). Li *et al.* (2001) and Zhang *et al.* (2002b) have introduced the piezoelectric effect and inverse piezoelectric effect in the 2-2 cement based piezoelectric composite with high sensitivity and output drive. Besides, Huang *et al.* (2004) have investigated the piezoelectric properties of the 0-3 PZT/sulfoaluminate cement composites and their dependences on the content of PZT and electrode conditions. Chaipanich (2007a, b) and Chaipanich *et al.* (2010) have further studied the influences of the constituents (Portland cement, silica fume cement, and PZT ceramic particle size etc.) on the dielectric, piezoelectric and the ferroelectric hysteresis properties of the 0-3 composite. Although being widely used due to the simple fabrication method, the general performance of the 0-3 cement-based piezoelectric composites can hardly meet the engineering requirements. Besides, Huang and Xu (2008) have also studied the dielectric and piezoelectric properties of 2-2 cement-based piezoelectric composite. Potong *et al.* (2012) have fabricated a 1-3 cement based piezoelectric material by mixing zirconate titanate (PZT) ceramic with Portland cement. The ferroelectric hysteresis behavior and the dielectric properties of the 1-3 lead zirconate titanate-cement composites have been studied. With the compacted method, Wang *et al.* (2012) have fabricated a 0-3 cement-based piezoelectric composite with superior piezoelectric properties. In others applications, a new type of cement-based piezoelectric sensor has been developed and investigated for monitoring the traffic flows by Li and Yang (2006). Good potential has been shown for the cement-based piezoelectric sensor in the engineering application for monitoring traffic flows in the field of transportation.

In contrast to intensive experimental work, the cement based piezoelectric composite is still not fully understood. The above mentioned works have focused on fabricating and testing the cement based piezoelectric composite. Only small amount literatures deal with the theoretical analysis of the cement based piezoelectric composite, especially for the 2-2, 0-3 and 1-3 cement based types. For example, the authors have performed the exact analysis of the dynamic properties of a 2-2 cement based piezoelectric flat transducer (Zhang and Shi 2011a, b) based on the previous work (Shi 2005, Shi and Zhang 2007). However, because of the complicated shape of bonding layer between the flat sensor/actuator and the curved surface of the host, it could be much more difficult to get precise information from a single test point. Therefore, this paper extends the exact analysis to the 2-2 cement based piezoelectric curved actuator considering the effect of the electrode layer.

The rest of the paper is organized as follows: In section 2, an analytical model consisting of piezoelectric/cement/electrode layers was established for the 2-2 cement based piezoelectric curved actuator. The actuator consists of one piezoelectric layer, two cement layers and two electrode layers. With the displacement method, the exact solutions are obtained for the displacement and stress of each layer under external electric signal in Section 3. Section 4 presents the comparisons and discussions between the numerical and analytical results, which agree well with each other. Furthermore, the influence of some parameters on the displacement and potential of the piezoelectric/cement layers are demonstrated, such as: the influence of the ratios S_{11E}/S_{33E} (considering the anisotropy/isotropy of the cement and electrode layer) and the layer thicknesses (especially that of the electrode layer); these parameters could be adjusted to obtain the desired displacements and stresses. Finally, the conclusions are given.

2. Basic model and formulae

Fig. 1 shows the schematic of a 2-2 cement-based piezoelectric curved composite with random θ . The basic layer model consists of five layers: a central piezoelectric layer (#3) is sandwiched between two outer cement layers (#1, #5) with two interfacial electrode layers (#2, #4). An external electrical potential V_0 is applied on the electrode layers. The thickness of the layer # i is derived as $(R_i - R_{i-1})$ ($i=1-5$). The strain, stress, induction and electric field are denoted by S_{ij} , T_{ij} , D_i and E_i , respectively. Without considering the body force/charge, the constitutive equations for the transversely isotropic elastic materials and piezoelectric materials subjected to a plane deformation can be written as

$$\begin{cases} S_\theta = S_{11E}T_\theta + S_{13E}T_r \\ S_r = S_{13E}T_\theta + S_{33E}T_r \\ S_{r\theta} = S_{44E}T_{r\theta} \end{cases} \quad (\text{for layers \#1, \#2, \#4, \#5}) \quad (1a)$$

$$\begin{cases} S_\theta = S_{11P}^D T_\theta + S_{13P}^D T_r + g_{31} D_r \\ S_r = S_{13P}^D T_\theta + S_{33P}^D T_r + g_{33} D_r \\ S_{r\theta} = S_{44P}^D T_{r\theta} + g_{15} D_\theta \\ E_\theta = -g_{15} T_{r\theta} + \beta_{11}^T D_\theta \\ E_r = -g_{31} T_\theta - g_{33} T_r + \beta_{33}^T D_r \end{cases} \quad (\text{for piezoelectric layer \#3}) \quad (1b)$$

where S_{klE} and S_{klP}^D are the coefficients of the effective elastic compliance for the elastic and piezoelectric layers; g_{kl} and β_{kl}^T are the coefficients of the piezoelectric and dielectric impermeability for the piezoelectric layers. The strain components for both elastic and piezoelectric materials can be expressed by means of the displacement components (u_r and u_θ) as

$$\begin{cases} S_\theta = \frac{u_r}{r} + \frac{1}{r} \frac{\partial u_\theta}{\partial \theta} \\ S_r = \frac{\partial u_r}{\partial r} \\ S_{r\theta} = \frac{1}{r} \frac{\partial u_r}{\partial \theta} + \frac{\partial u_\theta}{\partial r} - \frac{u_\theta}{r} \end{cases} \quad (2a)$$

For the piezoelectric materials, another set of geometrical equations for the electric field E and the electrical potential ϕ holds

$$\begin{cases} E_\theta = -\frac{1}{r} \frac{\partial \phi}{\partial \theta} \\ E_r = -\frac{\partial \phi}{\partial r} \end{cases} \quad (2b)$$

By ignoring the body force, the equilibrium equations for both elastic and piezoelectric materials hold

$$\begin{cases} \frac{\partial T_r}{\partial r} + \frac{1}{r} \frac{\partial T_{r\theta}}{\partial \theta} + \frac{T_r - T_\theta}{r} = 0 \\ \frac{\partial T_{r\theta}}{\partial r} + \frac{1}{r} \frac{\partial T_\theta}{\partial \theta} + \frac{2T_{r\theta}}{r} = 0 \end{cases} \quad (3a)$$

Moreover, by ignoring the body charge, the induction components of the piezoelectric materials should satisfy the following equilibrium equation

$$\frac{1}{r} \frac{\partial D_\theta}{\partial \theta} + \frac{D_r}{r} + \frac{\partial D_r}{\partial r} = 0 \quad (3b)$$

Besides, to ensure that the displacement can be derived by integrating the strain field, the strain components must satisfy the following compatibility equation

$$\left(\frac{\partial^2}{\partial r^2} + \frac{2}{r} \frac{\partial}{\partial r} \right) S_\theta + \left(\frac{1}{r^2} \frac{\partial^2}{\partial \theta^2} - \frac{1}{r} \frac{\partial}{\partial r} \right) S_r = \left(\frac{1}{r^2} \frac{\partial}{\partial \theta} + \frac{1}{r} \frac{\partial^2}{\partial r \partial \theta} \right) S_{r\theta} \quad (4)$$

Solutions of the above equations for the 2-2 cement-based piezoelectric curved composites considering the electrode layer will be discussed in the following sections.

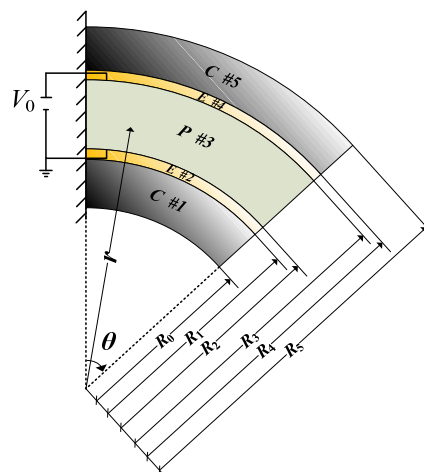


Fig. 1 Schematic of a 2-2 cement-based piezoelectric curved composite with random θ . (C, E and P denote cement layer, electrode layer and piezoelectric layer respectively)

3. Analytical solutions of 2-2 multi-layered piezoelectric curved composites

First, we consider the 2-2 cement-based piezoelectric curved composites with anisotropic cement layers and electrode layers. With the aid of the general theory of the piezo-elasticity and the previously obtained results (Shi and Zhang 2007), the expressions for each constituent layer are obtained as

$$\begin{cases} T_{\theta(i)} = C_{2(i)} - C_{3(i)}S_i r^{-S_i-1} + C_{4(i)}S_i r^{S_i-1} \\ T_{r(i)} = C_{2(i)} + C_{3(i)}r^{-S_i-1} + C_{4(i)}r^{S_i-1} \\ T_{r\theta(i)} = 0 \end{cases} \quad (i=1,2,4,5) \quad (5a)$$

$$\begin{cases} T_{\theta(3)} = C_{2(3)} - C_{3(3)}S_3 r^{-S_3-1} + C_{4(3)}S_3 r^{S_3-1} \\ T_{r(3)} = C_{2(3)} + C_{3(3)}r^{-S_3-1} + C_{4(3)}r^{S_3-1} - C_5 r^{-1} \\ E_r = -\frac{d\phi(r)}{dr}, \quad D_r = \frac{S_{33P} C_5}{g_{33} r} \\ E_\theta = 0, \quad D_\theta = 0, \quad T_{r\theta} = 0 \end{cases} \quad (i=3) \quad (5b)$$

$$\begin{cases} u_{r(i)} = e_{1(i)}C_{2(i)}r + e_{2(i)}C_{3(i)}r^{-S_i} + e_{3(i)}C_{4(i)}r^{S_i} + D_{1(i)}\cos\theta + D_{2(i)}\sin\theta \\ u_{\theta(i)} = e_{4(i)}C_{2(i)}r\theta + D_{2(i)}\cos\theta - D_{1(i)}\sin\theta + rD_{3(i)} \end{cases} \quad (i=1,2,4,5) \quad (6a)$$

$$\begin{cases} u_{r(3)} = e_{1(3)}C_{2(3)}r + e_{2(3)}C_{3(3)}r^{-S_3} + e_{3(3)}C_{4(3)}r^{S_3} - p_4 C_5 + D_{1(3)}\cos\theta + D_{2(3)}\sin\theta \\ u_{\theta(3)} = e_{4(3)}C_{2(3)}r\theta + D_{2(3)}\cos\theta - D_{1(3)}\sin\theta + rD_{3(3)} \\ \phi = p_6 C_{2(3)}r + p_7 C_{3(3)}r^{-S_3} + p_8 C_{4(3)}r^{S_3} - p_9 C_5 \ln r + C_6 \end{cases} \quad (i=3) \quad (6b)$$

in which

$$\begin{cases} e_{1(i)} = S_{33(i)} + S_{13(i)}, e_{2(i)} = S_{13(i)} - \frac{S_{33(i)}}{S_i}, e_{3(i)} = S_{13(i)} + \frac{S_{33(i)}}{S_i}, e_{4(i)} = S_{11(i)} - S_{33(i)} \\ e_{1(3)} = S_{33P} + S_{13P}, e_{2(3)} = S_{13P} - \frac{S_{33P}}{S_3}, e_{3(3)} = S_{13P} + \frac{S_{33P}}{S_3}, p_4 = S_{13P} - \frac{g_{31}S_{33P}}{g_{33}} \\ e_{4(3)} = S_{11P} - S_{33P}, p_6 = g_{31} + g_{33}, p_7 = g_{31} - \frac{g_{33}}{S_3}, p_8 = (g_{31} + \frac{g_{33}}{S_P}) \\ p_9 = g_{33} + \frac{S_{33P}\beta_{33}^T}{g_{33}}, S_i = \sqrt{\frac{S_{33(i)}}{S_{11(i)}}} \neq 1, S_3 = \sqrt{\frac{S_{33P}^D}{S_{11P}^D}}, \end{cases} \quad (i=1, 2, 4, 5) \quad (7)$$

where $C_{k(i)}$, $D_{l(i)}$, C_5 and C_6 ($i=1\sim 5$; $k=2\sim 4$; $l=1\sim 3$) are constants to be determined by using geometrical and electrical boundary conditions.

It is noticed that in deriving Eqs. (5) and (6), the term $((S_i - 1)^{-1} r^{S_i - 2})$ appears under the condition $S_i \neq 1$ (anisotropic). The isotropic case ($S_i=1, i=1, 2, 4, 5$) is considered by starting from Eqs. (1)-(4) and will be treated later in this section.

Eqs. (5) and (6) constitute one type of solutions of the above basic equations, which are used to study the bending behavior of the cement-based piezoelectric curved composite. To solve the equations, it is first noticed that the boundary conditions $(D_\theta|_{\theta=0} = D_\theta|_{\theta=\theta_0} = 0)$ are automatically satisfied. The boundary conditions of the electrical potential and stresses could be written as

$$\phi|_{r=R_3} = V_0 \tag{8a}$$

$$\phi|_{r=R_2} = 0 \tag{8b}$$

$$T_{r(5)}|_{r=R_3} = 0 \tag{9a}$$

$$T_{r(1)}|_{r=R_0} = 0 \tag{9b}$$

In full form, Eqs. (8) and (9) are

$$p_6 C_{2(3)} R_3 + p_7 C_{3(3)} R_3^{-S_3} + p_8 C_{4(3)} R_3^{S_3} - p_9 C_5 \ln R_3 + C_6 = V_0 \tag{10a}$$

$$p_6 C_{2(3)} R_2 + p_7 C_{3(3)} R_2^{-S_3} + p_8 C_{4(3)} R_2^{S_3} - p_9 C_5 \ln R_2 + C_6 = 0 \tag{10b}$$

$$C_{2(5)} + C_{3(5)} R_5^{-S_5 - 1} + C_{4(5)} R_5^{S_5 - 1} = 0 \tag{11a}$$

$$C_{2(1)} + C_{3(1)} R_0^{-S_1 - 1} + C_{4(1)} R_0^{S_1 - 1} = 0 \tag{11b}$$

In addition, the stress (T_r) and the displacements (u_r and u_θ) at all interfaces should be continuous, i.e.

$$T_{r(i)}|_{r=R_i} = T_{r(i+1)}|_{r=R_i} \tag{12}$$

$$u_{r(i)}|_{r=R_i} = u_{r(i+1)}|_{r=R_i}, \quad u_{\theta(i)}|_{r=R_i} = u_{\theta(i+1)}|_{r=R_i} \quad (1 \leq i \leq 4) \tag{13}$$

which leads to

$$\begin{cases} C_{2(i)} = a_{2(i)} C_{2(1)} \\ C_{3(i)} = \delta_{2(i)}^1 C_{2(1)} + \delta_{3(i)}^1 C_{3(1)} + \delta_{5(i)}^1 C_5 \\ C_{4(i)} = \delta_{2(i)}^2 C_{2(1)} + \delta_{3(i)}^2 C_{3(1)} + \delta_{5(i)}^2 C_5 \\ D_{1(i)} = D_1, \quad D_{2(i)} = D_2, \quad D_{3(i)} = D_3 \end{cases} \quad (1 \leq i \leq 5) \tag{14}$$

which shows that all $C_{k(i)}$ ($k = 2, 3, 4$) can be expressed in terms of $C_{2(i)}, C_{3(i)}$ and C_5 , respectively. To find a general solution and simplify the expressions, the following recurrence formulae are introduced

$$\begin{cases} \delta_{j(i)}^1 = \frac{\eta_{j(i)}^2 - \eta_{j(i)}^1 e_{3(i)}}{(e_{2(i)} - e_{3(i)})R_{i-1}^{-S_i-1}} \\ \delta_{j(i)}^2 = \frac{\eta_{j(i)}^2 - \eta_{j(i)}^1 e_{2(i)}}{(e_{3(i)} - e_{2(i)})R_{i-1}^{S_i-1}} \end{cases} \quad (j=2, 3, 5; 2 \leq i \leq 5) \quad (15a)$$

$$a_{2(i)} = \frac{e_{4(1)}}{e_{4(i)}} \quad (1 \leq i \leq 5) \quad (15b)$$

Here we suppose

$$\delta_{2(1)}^1 = \delta_{5(1)}^1 = \delta_{5(1)}^2 = \delta_{5(2)}^1 = \delta_{5(2)}^2 = 0, \delta_{3(1)}^1 = 1, \delta_{2(1)}^2 = -\frac{1}{R_0^{S_1-1}}, \delta_{3(1)}^2 = -R_0^{-2S_1} \quad (16)$$

where the superscripts 1 and 2 should not be confused with the layer number and: ($1 \leq i \leq 4$)

$$\eta_{2(i+1)}^1 = a_{2(i)} - a_{2(i+1)} + R_i^{-S_i-1} \delta_{2(i)}^1 + R_i^{S_i-1} \delta_{2(i)}^2 \quad (17a)$$

$$\eta_{2(i+1)}^2 = e_{1(i)} a_{2(i)} - e_{1(i+1)} a_{2(i+1)} + e_{2(i)} R_i^{-S_i-1} \delta_{2(i)}^1 + e_{3(i)} R_i^{S_i-1} \delta_{2(i)}^2 \quad (17b)$$

$$\eta_{3(i+1)}^1 = R_i^{-S_i-1} \delta_{3(i)}^1 + R_i^{S_i-1} \delta_{3(i)}^2 \quad (17c)$$

$$\eta_{3(i+1)}^2 = e_{2(i)} R_i^{-S_i-1} \delta_{3(i)}^1 + e_{3(i)} R_i^{S_i-1} \delta_{3(i)}^2 \quad (17d)$$

$$\eta_{5(3)}^1 = R_2^{-1}, \eta_{5(3)}^2 = R_2^{-1} p_4 \quad (17e)$$

$$\eta_{5(l+1)}^1 = R_l^{-S_l-1} \delta_{5(l)}^1 + R_l^{S_l-1} \delta_{5(l)}^2 - b_0 R_l^{-1} \quad (17f)$$

$$\eta_{5(l+1)}^2 = e_{2(l)} R_l^{-S_l-1} \delta_{5(l)}^1 + e_{3(l)} R_l^{S_l-1} \delta_{5(l)}^2 - b_0 R_l^{-1} p_4 \quad (17g)$$

Here, the index l takes either 3 ($b_0 = 1$) or 4 ($b_0 = 0$).

In order to satisfy the mechanical boundary conditions at the free end, the Saint-Venant's principle is considered, which leads to the following two equations

$$\int_{R_0}^{R_5} T_\theta dr = 0 \quad , \quad \int_{R_0}^{R_5} T_\theta \cdot r dr = 0 \quad (18)$$

where, the first equation is satisfied automatically. By substituting Eq. (14) into Eqs. (10), (11a) and the second equation of (18), $C_{2(i)}, C_{3(i)}, C_5$ and C_6 can be determined as

$$C = H^{-1}L \tag{19}$$

with

$$C = \begin{Bmatrix} C_{2(i)} \\ C_{3(i)} \\ C_5 \\ C_6 \end{Bmatrix}, \quad H = \begin{pmatrix} h_{11} & h_{12} & h_{13} & 0 \\ h_{21} & h_{22} & h_{23} & 1 \\ h_{31} & h_{32} & h_{33} & 1 \\ h_{41} & h_{42} & h_{43} & 0 \end{pmatrix}, \quad L = \begin{Bmatrix} 0 \\ 0 \\ V_0 \\ 0 \end{Bmatrix} \tag{20}$$

Here, we define

$$\begin{cases} h_{11} = \sum_{i=1}^5 \left[\frac{1}{2} (R_i^2 - R_{i-1}^2) a_{2(i)} - \frac{S_i}{-S_i + 1} (R_i^{-S_i+1} - R_{i-1}^{-S_i+1}) \delta_{2(i)}^1 + \frac{S_i}{S_i + 1} (R_i^{S_i+1} - R_{i-1}^{S_i+1}) \delta_{2(i)}^2 \right] \\ h_{12} = \sum_{i=1}^5 -\frac{S_i}{-S_i + 1} (R_i^{-S_i+1} - R_{i-1}^{-S_i+1}) \delta_{3(i)}^1 + \frac{S_i}{S_i + 1} (R_i^{S_i+1} - R_{i-1}^{S_i+1}) \delta_{3(i)}^2 \\ h_{13} = \sum_{i=1}^5 -\frac{S_i}{-S_i + 1} (R_i^{-S_i+1} - R_{i-1}^{-S_i+1}) \delta_{5(i)}^1 + \frac{S_i}{S_i + 1} (R_i^{S_i+1} - R_{i-1}^{S_i+1}) \delta_{5(i)}^2 \end{cases} \tag{21a}$$

$$\begin{cases} h_{11} = p_6 a_{23} R_i + p_7 \delta_{23}^1 R_i^{-S_3} + p_8 \delta_{23}^2 R_i^{S_3} \\ h_{12} = p_7 \delta_{33}^1 R_i^{-S_3} + p_8 \delta_{33}^2 R_i^{S_3} \\ h_{13} = p_7 \delta_{53}^1 R_i^{-S_3} + p_8 \delta_{53}^2 R_i^{S_3} - p_9 \ln R_i \end{cases} \quad (i=2, 3) \tag{21b}$$

$$\begin{cases} h_{41} = a_{2(5)} + R_5^{-S_5-1} \delta_{25}^1 + R_5^{S_5-1} \delta_{25}^2 \\ h_{42} = R_5^{-S_5-1} \delta_{35}^1 + R_5^{S_5-1} \delta_{35}^2 \\ h_{43} = R_5^{-S_5-1} \delta_{55}^1 + R_5^{S_5-1} \delta_{55}^2 \end{cases} \tag{21c}$$

By substituting Eq. (19) into Eq. (14), all the unknown constants $C_{k(i)}$, C_5 and C_6 can be determined. To determine the unknown constants D_i ($i=1, 2,$ and 3) in u_r and u_θ , the following geometric constraints will be considered

$$u_r(R_{00}, 0) = 0 \quad , \quad u_\theta(R_{00}, 0) = 0 \quad , \quad \frac{\partial u_r(R_{00}, 0)}{\partial \theta} = 0 \tag{22}$$

with $R_{00} = (R_5 + R_0) / 2$.

As a result, D_i ($i=1\sim 3$) are deduced to be

$$\begin{cases} D_1 = -p_1 C_{2(3)} R_{00} - p_2 C_{3(3)} R_{00}^{-S_3} - p_3 C_{4(3)} R_{00}^{S_3} + p_4 C_5 \\ D_2 = 0 \\ D_3 = 0 \end{cases} \quad (23)$$

Up to now, the exact mechanical and electrical fields of the 2-2 multi-layered piezoelectric curved composites are fully determined with the anisotropic cement and electrode layers .

When considering the isotropic cement and electrode layers, one starts from Eqs. (1)-(4) and assumes that $S_{(i)}=1$ ($i=1, 2, 4, 5$, see Eq. (7) for definition), the stress components in the elastic layers are solved to be

$$\begin{cases} T_{\theta(i)} = C_{2(i)} - C_{3(i)} r^{-2} + (2 \ln r + 3) C_{4(i)} \\ T_{r(i)} = C_{2(i)} + C_{3(i)} r^{-2} + (2 \ln r + 1) C_{4(i)} \\ T_{r\theta(i)} = 0 \end{cases} \quad (i=1, 2, 4, 5) \quad (24)$$

It is noticed that Eq. (24) can not be obtained by simply substituting $S_{(i)}=1$ ($i=1, 2, 4, 5$) into Eqs. (5) and (6). The 2-2 cement-based piezoelectric curved composites with isotropic cement layers and electrode layers are studied and the exact solutions can be found in Appendix A for clarity.

Furthermore, using the same procedure, the exact solutions of 2-2 cement-based piezoelectric curved composites with anisotropic cement layers and isotropic electrode layers can also be deduced, further details are not listed here for simplicity.

4. Numerical results and comparisons

In previous sections, the exact solutions of 2-2 cement-based piezoelectric curved composites considering the electrode layers with anisotropic or isotropic elastic layers have been obtained. Numerical analysis is presented in this section for comparison. To be specific and unless otherwise pointed out, the thickness of each cement layer, electrode layer and piezoelectric layer takes the value $h_c = 0.25 \text{ mm}$, $h_e = 0.05 \text{ mm}$ and $h_p = 0.4 \text{ mm}$, respectively. The inner radius of the curved composite R_1 is taken as 16 mm . The electrode layers are made of (Gold-tin, 80 wt.% Au - 20 wt.% Sn) (Rassaian and Beranek 1999), with the elastic modulus and Poisson's ratio of 137.3 GPa and 0.3, respectively. For the piezoelectric layers made of PZT-4, the material parameters are listed in Table 1 which is transformed from Table 2 in Ref. (Ruan *et al.* 2000). The ratios $S_{11E(i)} / S_{33E(i)}$ ($i=1, 2, 4, 5$) are assumed to be the same and constant (for short as S_{11E} / S_{33E}) in the numerical calculation in the following figures.

Based on the exact solutions obtained in the last section, Figs. 2-5 show, respectively, the dependences of normal stresses (T_θ, T_r), electrical potential ϕ and induction D_r on the radius r for different values of S_{11E} / S_{33E} . It is found that the normal stresses (T_θ, T_r) in each layer decrease as S_{11E} / S_{33E} increases. The stress T_r is much smaller compared to T_θ , thus can be neglected especially when $S_{11E} > S_{33E}$. However, S_{11E} / S_{33E} has minor influence on the distribution of ϕ , the slopes of T_θ and D_r in the composite. That is to say, ϕ changes almost

linearly in the radial direction and T_θ and D_r are almost parallel to each other for different values of S_{11E}/S_{33E} . Figs. 2-5 show that the desired normal stresses could be obtained by changing the value of S_{11E}/S_{33E} in designing the actuator.

Table 1 Material constants of PZT-4 (For model-g constitutive relations)

Elastic constant (10^{-12} m ² /N)				Piezoelectric constant (10^{-3} m ² /C)			Dielectric impermeability constant (10^6 m/F)	
S_{11}^D	S_{13}^D	S_{33}^D	S_{44}^D	g_{31}	g_{33}	g_{15}	β_{11}^T	β_{33}^T
7.95	-3.03	7.91	17.91	-17.8	23.91	40.36	76.87	99.65

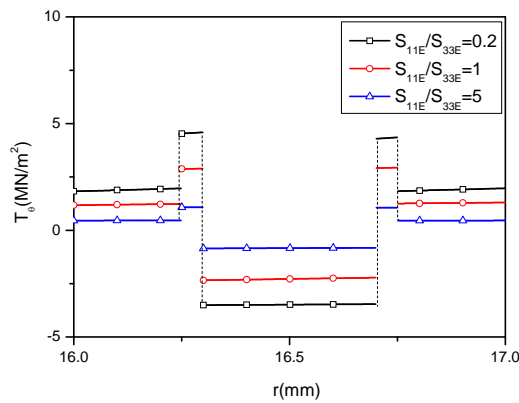


Fig. 2 Relation of normal stress T_θ versus radius r at $V_0=100$ V

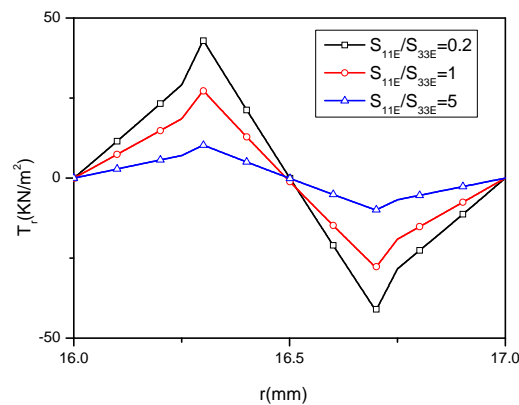


Fig. 3 Relation of normal stress T_r versus radius r at $V_0=100$ V

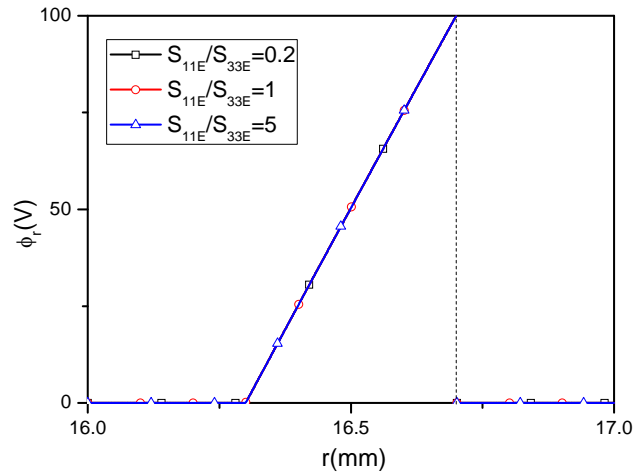


Fig. 4 Relation of electrical potential ϕ versus radius r

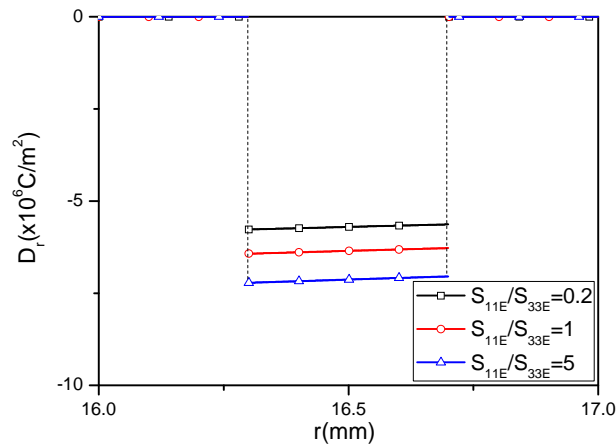


Fig. 5 Relation of induction D_r versus radius r at $V_0=100$ V

The displacements (u_r, u_θ) at the center of the layer #3 are plotted as a function of the angle θ in Figs. 6 and 7 according to the present analytical solution and numerical results. Good agreement is achieved. From Figs. 6 and 7, the largest displacements u_r, u_θ are obtained when $S_{11E}/S_{33E} = 1$. This indicates that, we can have the largest displacement if the cement/electrode

layers are isotropic; for anisotropic cement/electrode layers, the larger S_{11E}/S_{33E} results in smaller u_r and larger u_θ . Moreover, as S_{11E}/S_{33E} decreases in Fig.6 and increases in Fig. 7, u_r (u_θ) approaches a constant value smaller than that at $S_{11E}/S_{33E} = 1$. Therefore, the isotropic case is preferred, as the actuator will benefit from the larger range of displacement for braking.

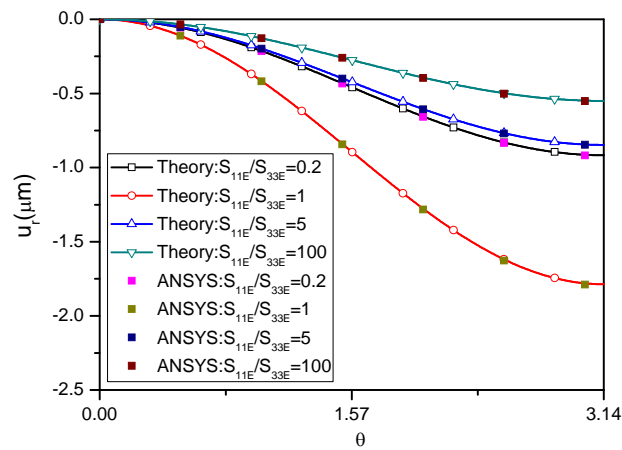


Fig. 6 Displacement u_r at the interface (or middle layer) of the composite as a function of angle θ at $V_0=100$ V

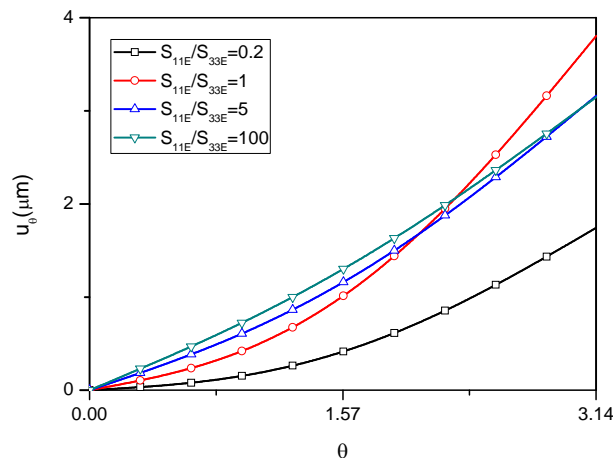


Fig. 7 Displacement u_θ at the interface (or middle layer) of the composite as a function of the angle θ at $V_0=100$ V

Assuming that the total thickness of the composite as well as that of the #3 layer is constant, Figs. 8 and 9 show the effect of the cement layer thickness on the distribution of (T_r, u_r) . Figs. 10 and 11 present the distribution of (T_r, u_r) over the thickness ratio h_c/h_p (h_E is constant). We notice that the smaller the ratio h_c/h_E is, the larger the displacements and the internal stress become; on the other hand, the larger the ratios h_c/h_p are, the larger the displacements and the internal stress become. This indicates that thinner electrode layers are preferable for the composite. When the thickness of the cement layer h_c approaches zero, the results obtained here are consistent with those given in our previous work, which are layered piezoelectric composite with electrode layers (Shi and Zhang 2007).

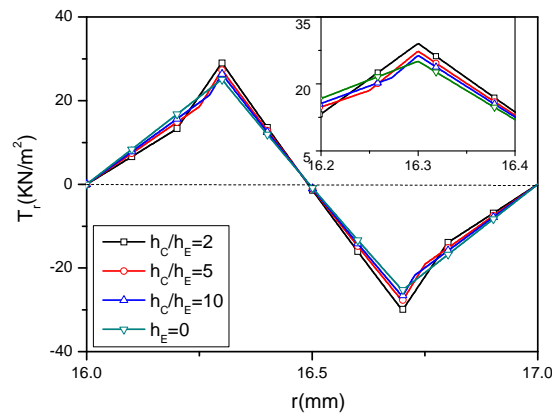


Fig. 8 Relation of normal stress T_r versus radius r for different values of h_c/h_E at $V_0=100$ V

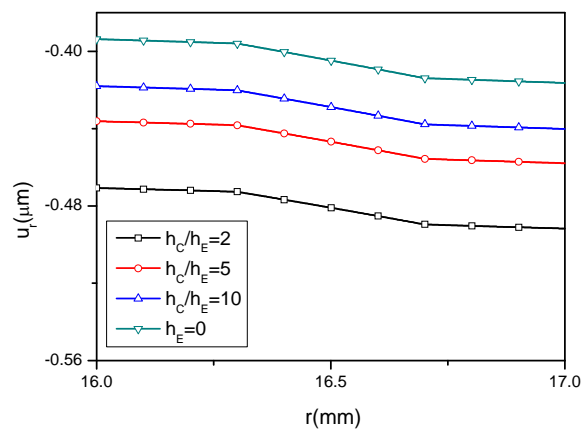


Fig. 9 Relation of displacement u_r versus radius r for different values of h_c/h_E at $V_0=100$ V

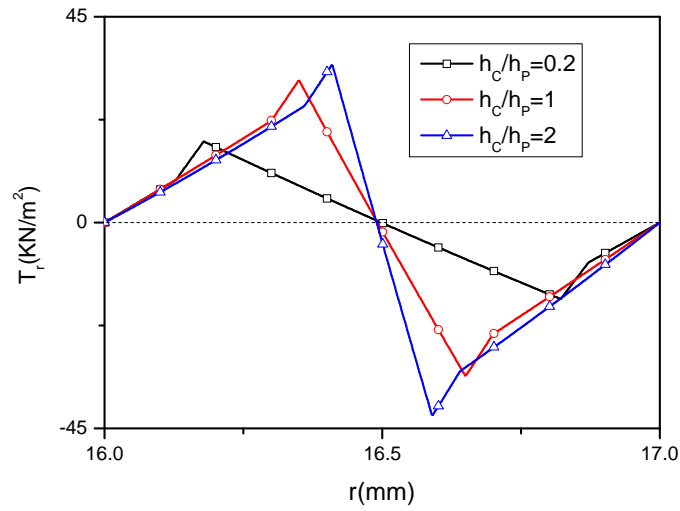


Fig. 10 Relation of normal stress T_r versus radius r for different values of h_c/h_p at $V_0=100$ V

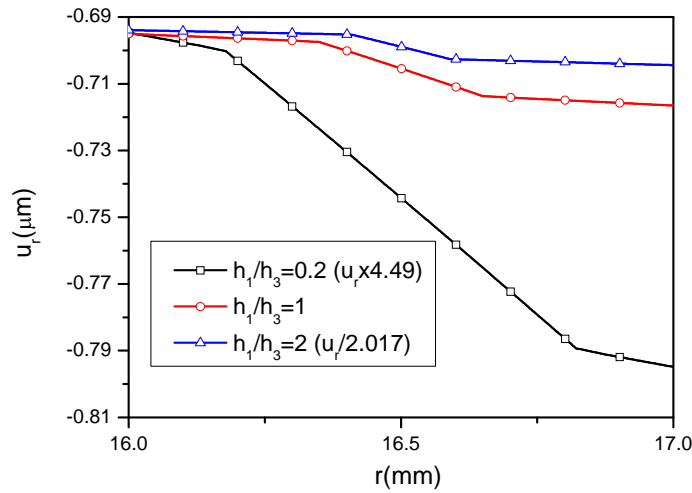


Fig. 11 Relation of displacement u_r versus radius r for different values of h_c/h_p at $V_0=100$ V

5. Conclusions

Based on the theory of piezoelectric elasticity, the analytical solutions of the 2-2 cement-based piezoelectric curved composites are presented with the consideration of the effect of the electrode layers. Both anisotropic and isotropic cement and electrode layers are investigated. It was found that:

- The desired normal stresses could be achieved by changing the value of S_{11E}/S_{33E} in designing the actuator;
- The distribution of the electrical potential ϕ , the slopes of stress T_θ and induction D_r in the composite are independent with S_{11E}/S_{33E} ;
- The isotropic case is preferred when the actuator requires large displacement range for braking;
- Thinner electrode layers are preferred for the composite;
- The present results could be readily used to model and design this type of cement-based piezoelectric curved actuators with random θ .

Acknowledgements

This work is supported by the National Natural Science Foundation of China (51278517). Support is also supplied by and the Fundamental Research Funds for the Central Universities (303347 and 30365501).

References

- Chaipanich, A. (2007a), "Dielectric and piezoelectric properties of PZT/cement composites", *Curr. Appl. Phys.*, **7**, 537-539.
- Chaipanich, A. (2007b), "Effect of PZT particle size on dielectric and piezoelectric properties of PZT-cement composites", *Curr. Appl. Phys.*, **7**, 574-577.
- Chaipanich, A., Rujijanagul, G. and Tunkasiri, T. (2010), "Effect of compressive stress on the ferroelectric hysteresis behavior in 0-3 PZT-cement composites", *Mater. Lett.*, **64**(5), 562-564.
- Huang, S.F., Chang, J. and Xu, R.H. (2004), "Piezoelectric properties of 0-3 PZT/sulfoaluminate cement composites", *Smart Mater. Struct.*, **13**(2), 270-274.
- Huang, S.F. and Xu, D.Y. (2008), "Dielectric and piezoelectric properties of 2-2 cement based piezoelectric composite", *J. Compos. Mater.*, **42**(23), 2437-2443.
- Li, Z. and Yang, X. (2006), "Application of cement-based piezoelectric sensors for monitoring traffic flows", *J. Transp. Eng. - ASCE*, **132**(7), 565-573.
- Li, Z.J., Zhang, D. and Wu, K.R. (2001), "Cement matrix 2-2 piezoelectric composite: Part I. Sensory effect", *Mater. Struct.*, **13**(242), 506-512.
- Li, Z.J., Zhang, D. and Wu, K.R. (2002), "Cement-based 0-3 piezoelectric composites", *J. Am. Ceramic Soc.*, **85**(2), 305-313.
- Potong, R., Rianyai, R., Jaitanong, N., Yimnirun, R. and Chaipanich, A. (2012), "Ferroelectric hysteresis behavior and dielectric properties of 1-3 lead zirconate titanate-cement composites", *Ferroelectrics letters section*, **39**(1), 15-19.
- Rassaian, M. and Beranek, M.W. (1999), "Quantitative Characterization of 96.5Sn3.5Ag and 80Au20Sn

- Optical Fiber Solder Bond Joints on Silicon Micro-Optical Bench Substrates”, *IEEE T. Adv. Packaging*, **22**(1), 86-93.
- Ruan, X.P., Danforth, S.S., Safari, A. and Chou, T.W. (2000), “Saint-Venant end effects in piezoceramic materials”, *Int. J. Solids. Struct.*, **37**, 2625-2637.
- Shi, Z.F. (2005), “Bending behavior of piezoelectric curved actuator”, *Smart Mater. Struct.*, **14**(4), 835-842.
- Shi, Z.F. and Zhang, T.T. (2007), “Static analyses for 2-2 multi-layered piezoelectric curved composites”, *Int. J. Eng. Sci.*, **45**, 509-524.
- Xu, D.Y., Chen, X., Huang, S.F. and Jiang, M.H. (2009), “Electromechanical properties of 2-2 cement based piezoelectric composite”, *Curr. Appl. Phys.*, **9**, 816-819.
- Wang, F.Z., Wang, H., Song, Y. And Sun, H.J. (2012), “High piezoelectricity 0-3 cement-based piezoelectric composites”, *Mater. Lett.*, **76**, 208-210.
- Xu, D.Y., Cheng, X., Huang, S.F. and Jiang, M.H. (2011), “Effect of cement matrix and composite thickness on properties of 2-2 type cement-based piezoelectric composites”, *J. Compos. Mater.*, **45**(20), 2083-2089.
- Zhang, D., Li, Z.J. and Wu, K.R. (2002a), “2-2 piezoelectric cement matrix composite: Part II. Actuator effect”, *Cement Concrete Res.*, **32**(5), 825-830.
- Zhang, D., Wu, K.R. and Li, Z.J. (2002b), “Feasibility study of cement based piezoelectric composite”, *J. Build. Mater.*, **5**(2), 141-146.
- Zhang, T.T. and Shi, Z.F. (2011a), “Exact analysis of the dynamic properties of a 2-2 cement based piezoelectric transducer”, *Smart Mater. Struct.*, **20**(8), 085017.
- Zhang, T.T. and Shi, Z.F. (2011b), “Exact solutions of the piezoelectric transducer under multi loads”, *Smart Struct. Syst.*, **8**(4), 413-431.

Appendix A:

For 2-2 multi-layered piezoelectric curved composites with the isotropic cement and electrode layers, the expressions for the *i*-th piezoelectric layer (5b) and (6b) are still valid. However, the expressions (5a) and (6a) for the *i*-th elastic layer are different and reads

$$\begin{cases} T_{\theta(i)} = C_{2(i)} - C_{3(i)}r^{-2} + (2\ln r + 3)C_{4(i)} \\ T_{r(i)} = C_{2(i)} + C_{3(i)}r^{-2} + (2\ln r + 1)C_{4(i)} \\ T_{r\theta(i)} = 0 \end{cases} \quad (A1)$$

$$\begin{cases} u_{r(i)} = e_{1(i)}C_{2(i)}r + e_{2(i)}C_{3(i)}r^{-1} + [e_{3(i)} + e_{5(i)}\ln r]rC_{4(i)} + D_{1(i)}\cos\theta + D_{2(i)}\sin\theta \\ u_{\theta(i)} = e_{4(i)}C_{4(i)}r\theta + D_{2(i)}\cos\theta - D_{1(i)}\sin\theta + rD_{3(i)} \end{cases} \quad (A2)$$

where $C_{k(i)}$, and $D_{l(i)}$ ($i=1, 2, 4, 5; k=2 \sim 4; l=1 \sim 3$) are constants to be determined. And

$$\begin{cases} e_{1(i)} = S_{13(i)} + S_{11(i)} \\ e_{2(i)} = S_{13(i)} - S_{11(i)} \\ e_{3(i)} = S_{13(i)} - S_{11(i)} \\ e_{4(i)} = 4S_{11(i)} \\ e_{5(i)} = 2(S_{13(i)} + S_{11(i)}) \end{cases} \quad (i=1, 2, 4, 5) \quad (A3)$$

Using the same procedure and considering the mechanical and electric boundary conditions, all the governing equations for determining the unknown constants can be obtained. Eq. (8) is still valid. Eq. (14) becomes

$$\begin{cases} C_{2(i)} = \delta_{3(i)}^1 C_{3(1)} + \delta_{4(i)}^1 C_{4(1)} + \delta_{5(i)}^1 C_5 \\ C_{3(i)} = \delta_{3(i)}^2 C_{3(1)} + \delta_{4(i)}^2 C_{4(1)} + \delta_{5(i)}^2 C_5 \\ C_{4(i)} = a_{4(i)} C_{4(1)} \\ D_{1(i)} = D_1, \quad D_{2(i)} = D_2, \quad D_{3(i)} = D_3 \end{cases} \quad (i=1, 2, 4, 5) \quad (A3a)$$

$$\begin{cases} C_{2(3)} = a_{4(3)} C_{4(1)} \\ C_{3(3)} = \delta_{3(3)}^1 C_{3(1)} + \delta_{4(3)}^1 C_{4(1)} + \delta_{5(3)}^1 C_5 \\ C_{4(3)} = \delta_{3(3)}^2 C_{3(1)} + \delta_{4(3)}^2 C_{4(1)} + \delta_{5(3)}^2 C_5 \\ D_{1(3)} = D_1, \quad D_{2(3)} = D_2, \quad D_{3(3)} = D_3 \end{cases} \quad (i=3) \quad (A3b)$$

Here we have for the elastic and cement layers: ($i=2, 4, 5$)

$$\begin{cases} \delta_{j(i)}^1 = \frac{\eta_{j(i)}^1 - \eta_{j(i)}^2 e_{2(i)} R_{i-1}}{(e_{1(i)} - e_{2(i)}) R_{i-1}} \\ \delta_{j(i)}^2 = \frac{\eta_{j(i)}^1 - \eta_{j(i)}^2 e_{1(i)} R_{i-1}}{(e_{2(i)} - e_{1(i)}) R_{i-1}^{-1}} \end{cases} \quad (j=3, 4, 5) \quad (\text{A4a})$$

and for piezoelectric layer.

$$\begin{cases} \delta_{j(3)}^1 = \frac{\eta_{j(3)}^1 - \eta_{j(3)}^2 e_{3(3)} R_2}{(e_{2(3)} - e_{3(3)}) R_2^{-S_3}} \\ \delta_{j(3)}^2 = \frac{\eta_{j(3)}^1 - \eta_{j(3)}^2 e_{2(3)} R_2}{(e_{3(3)} - e_{2(3)}) R_2^{S_3}} \end{cases} \quad (j=3, 4, 5) \quad (\text{A4b})$$

$$a_{4(i)} = \frac{e_{4(1)}}{e_{4(i)}} \quad (1 \leq i \leq 5) \quad (\text{A4c})$$

Moreover, $C_{3(1)}, C_{4(1)}, C_5$ and C_6 can be determined by

$$C' = H'^{-1} L' \quad (\text{A5})$$

in which

$$C' = \begin{Bmatrix} C_{3(1)} \\ C_{4(1)} \\ C_5 \\ C_6 \end{Bmatrix}, \quad H' = \begin{pmatrix} h'_{11} & h'_{12} & h'_{13} & 0 \\ h'_{21} & h'_{22} & h'_{23} & 1 \\ h'_{31} & h'_{32} & h'_{33} & 1 \\ h'_{41} & h'_{42} & h'_{43} & 0 \end{pmatrix}, \quad L' = \begin{Bmatrix} 0 \\ 0 \\ V_0 \\ 0 \end{Bmatrix} \quad (\text{A6})$$

Here we suppose

$$\delta_{5(1)}^1 = \delta_{5(1)}^2 = \delta_{4(1)}^2 = 0, \quad \delta_{3(1)}^2 = 1, \quad \delta_{3(1)}^1 = -\frac{1}{R_0^2}, \quad \delta_{4(1)}^1 = -2 \ln R_0 - 1 \quad (\text{A7})$$

in which superscripts 1 and 2 are symbols and the following symbols are used

$$\begin{cases} \eta_{3(2)}^1 = e_{1(1)} R_1 \delta_{3(1)}^1 + e_{2(1)} R_1^{-1} \\ \eta_{3(2)}^2 = \delta_{3(1)}^1 + R_1^{-2} \delta_{3(1)}^2 \\ \eta_{4(2)}^1 = (e_{1(1)} \delta_{4(1)}^1 + (e_{3(1)} + e_{5(1)}) a_{41} \ln R_1 - (e_{3(2)} + e_{5(2)} \ln R_1) a_{4(2)}) R_1 \\ \eta_{4(2)}^2 = \delta_{4(1)}^1 + (2 \ln R_1 + 1)(a_{41} - a_{4(2)}) \\ \eta_{5(2)}^1 = 0 \\ \eta_{5(2)}^2 = 0 \end{cases} \quad (\text{A8a})$$

$$\left\{ \begin{array}{l} \eta_{3(3)}^1 = e_{1(2)} R_2 \delta_{3(2)}^1 + e_{2(2)} R_2^{-1} \delta_{3(2)}^2 \\ \eta_{3(3)}^2 = \delta_{3(2)}^1 + R_2^{-2} \delta_{3(2)}^2 \\ \eta_{4(3)}^1 = (e_{1(2)} \delta_{4(2)}^1 + e_{2(2)} \delta_{4(2)}^2 R_2^{-2} + (e_{3(2)} + e_{5(2)} \ln R_2) a_{42} - e_{1(3)} a_{4(3)}) R_2 \\ \eta_{4(3)}^2 = \delta_{4(2)}^1 + \delta_{4(2)}^2 R_2^{-2} + (2 \ln R_2 + 1) a_{4(2)} - a_{4(3)} \\ \eta_{5(3)}^1 = -p_4 \\ \eta_{5(3)}^2 = R_2^{-1} \end{array} \right. \quad (\text{A8b})$$

$$\left\{ \begin{array}{l} \eta_{3(4)}^1 = e_{2(3)} R_3^{-S_3} \delta_{3(3)}^1 + e_{3(3)} R_3^{S_3} \delta_{3(3)}^2 \\ \eta_{3(4)}^2 = R_3^{-S_3-1} \delta_{3(3)}^1 + R_3^{S_3-1} \delta_{3(3)}^2 \\ \eta_{4(4)}^1 = (e_{1(3)} a_{4(3)} - (e_{3(4)} + e_{5(4)} \ln R_3) a_{4(4)}) R_3 + e_{2(3)} R_3^{-S_3} \delta_{4(3)}^1 + e_{3(3)} R_3^{S_3} \delta_{4(3)}^2 \\ \eta_{4(4)}^2 = a_{4(3)} - (2 \ln R_3 + 1) a_{4(4)} + R_3^{-S_3-1} \delta_{4(3)}^1 + R_3^{S_3-1} \delta_{4(3)}^2 \\ \eta_{5(4)}^1 = e_{2(3)} R_3^{-S_3} \delta_{5(3)}^1 + e_{3(3)} R_3^{S_3} \delta_{5(3)}^2 - p_4 \\ \eta_{5(4)}^2 = R_3^{-S_3-1} \delta_{5(3)}^1 + R_3^{S_3-1} \delta_{5(3)}^2 - R_3^{-1} \end{array} \right. \quad (\text{A8c})$$

$$\left\{ \begin{array}{l} \eta_{3(5)}^1 = e_{1(4)} R_4 \delta_{3(4)}^1 + e_{2(4)} R_4^{-1} \delta_{3(4)}^2 \\ \eta_{3(5)}^2 = \delta_{3(4)}^1 + R_4^{-2} \delta_{3(4)}^2 \\ \eta_{4(5)}^1 = e_{1(4)} R_4 \delta_{4(4)}^1 + e_{2(4)} R_4^{-1} \delta_{4(4)}^2 + (e_{3(4)} + e_{5(4)} \ln R_4) R_4 a_{4(4)} - (e_{3(5)} + e_{5(5)} \ln R_4) R_4 a_{4(5)} \\ \eta_{4(5)}^2 = \delta_{4(4)}^1 + \delta_{4(4)}^2 R_4^{-2} + (2 \ln R_4 + 1) (a_{4(4)} - a_{4(5)}) \\ \eta_{5(5)}^1 = e_{1(4)} R_4 \delta_{5(4)}^1 + e_{2(4)} R_4^{-1} \delta_{5(4)}^2 \\ \eta_{5(5)}^2 = \delta_{5(4)}^1 + R_4^{-2} \delta_{5(4)}^2 \end{array} \right. \quad (\text{A8d})$$

where

$$\left\{ \begin{aligned} h_{11} &= \sum_{i=1,2,4,5} \left[\left(\frac{R_i^2 - R_{i-1}^2}{2} \right) \delta_{3(i)}^1 - \ln \frac{R_i}{R_{i-1}} \delta_{3(i)}^2 \right] + \sum_{j=1}^2 m_j \delta_{3(3)}^j \\ h_{12} &= \sum_{i=1,2,4,5} \left[\left(\frac{R_i^2 - R_{i-1}^2}{2} \right) \delta_{4(i)}^1 - \ln \frac{R_i}{R_{i-1}} \delta_{4(i)}^2 + a_{4(i)} (R_i^2 (\ln R_i + 1) - R_{i-1}^2 (\ln R_{i-1} + 1)) \right] \\ &\quad + \frac{R_3^2 - R_2^2}{2} a_{4(3)} + \sum_{j=1}^2 m_j \delta_{4(3)}^j \\ h_{13} &= \sum_{i=1,2,4,5} \left[\left(\frac{R_i^2 - R_{i-1}^2}{2} \right) \delta_{5(i)}^1 - \ln \frac{R_i}{R_{i-1}} \delta_{5(i)}^2 \right] + \sum_{j=1}^2 m_j \delta_{5(3)}^j \\ m_1 &= -\frac{S_3}{-S_3 + 1} (R_3^{-S_3+1} - R_2^{-S_3+1}), m_2 = \frac{S_3}{S_3 + 1} (R_3^{S_3+1} - R_2^{S_3+1}), \end{aligned} \right. \tag{A9a}$$

$$\left\{ \begin{aligned} h_{i1} &= p_7 \delta_{33}^1 R_i^{-S_3} + p_8 \delta_{33}^2 R_i^{S_3} \\ h_{i2} &= p_6 a_{4(3)} R_i + p_7 \delta_{43}^1 R_i^{-S_3} + p_8 \delta_{43}^2 R_i^{S_3} \\ h_{i3} &= p_7 \delta_{53}^1 R_i^{-S_3} + p_8 \delta_{53}^2 R_i^{S_3} - p_9 \ln R_i \end{aligned} \right. \quad (i=2, 3) \tag{A9b}$$

$$\left\{ \begin{aligned} h_{41} &= \delta_{35}^1 + R_5^{-2} \delta_{35}^2 \\ h_{42} &= \delta_{45}^1 + R_5^{-2} \delta_{45}^2 + (2 \ln R_5 + 1) a_{4(5)} \\ h_{43} &= \delta_{55}^1 + R_5^{-2} \delta_{55}^2 \end{aligned} \right. \tag{A9c}$$

$$\left\{ \begin{aligned} D_1 &= -e_{1(3)} C_{2(3)} R_{00} - e_{2(3)} C_{3(3)} R_{00}^{-S_3} - e_{3(3)} C_{4(3)} R_{00}^{S_3} + p_4 C_5 \\ D_2 &= 0 \\ D_3 &= 0 \end{aligned} \right. \tag{A10}$$

Till now, all the unknown parameters have been determined.